



Exchange bias at the organic/ferromagnet interface may not be a spinterface effect

Garen Avedissian, Jacek Arabski, Jennifer A Wytko, Jean Weiss, Vasiliki Papaefthimiou, Guy Schmerber, Guillaume Rogez, Eric Beaurepaire, Christian Meny

► To cite this version:

Garen Avedissian, Jacek Arabski, Jennifer A Wytko, Jean Weiss, Vasiliki Papaefthimiou, et al.. Exchange bias at the organic/ferromagnet interface may not be a spinterface effect. *Applied Physics Reviews*, 2022, 9 (1), pp.011417. 10.1063/5.0054524 . hal-03582523

HAL Id: hal-03582523

<https://hal.science/hal-03582523>

Submitted on 21 Feb 2022

HAL is a multi-disciplinary open access archive for the deposit and dissemination of scientific research documents, whether they are published or not. The documents may come from teaching and research institutions in France or abroad, or from public or private research centers.

L'archive ouverte pluridisciplinaire **HAL**, est destinée au dépôt et à la diffusion de documents scientifiques de niveau recherche, publiés ou non, émanant des établissements d'enseignement et de recherche français ou étrangers, des laboratoires publics ou privés.

Exchange bias at the organic/ferromagnet interface may not be a spinterface effect

Garen Avedissian,^{1*†} Jacek Arabski,¹ Jennifer A. Wytko,² Jean Weiss,² Vasiliki Papaefthimiou,³ Guy Schmerber,¹ Guillaume Rogez,¹ Eric Beaurepaire,^{1†} and Christian Meny^{1*}

¹*Institut de Physique et Chimie des Matériaux de Strasbourg, Université de Strasbourg, CNRS UMR 7504, 23 rue de Loess, BP 43, F-67034 Strasbourg Cedex 2, France*

²*Institut de Chimie de Strasbourg, Université de Strasbourg, CNRS UMR 7177, 4 rue Blaise Pascal, F-67081 Strasbourg Cedex, France*

³*Institut de Chimie et Procédés pour l'Energie, l'Environnement et la Sante, Université De Strasbourg, CNRS UMR 7515, 25 rue Becquerel, F-67087 Strasbourg Cedex 2, France*

*Corresponding authors: christian.meny@ipcms.unistra.fr and garen.avedissian@ipcms.unistra.fr

‡ Present address: CIC nanoGUNE BRTA, Tolosa Hiribidea, 76, 20018 Donostia, San Sebastian, Spain

† Deceased April 24th, 2018

ABSTRACT

Exchange bias is a physical effect that is used in many spintronic devices like magnetic read heads, MRAMS, and most kinds of magnetic sensors. For the next generation of fully organic devices, molecular exchange bias, if existing, could have a huge impact for developing mechanically soft and environment friendly devices. The observation of molecular exchange bias has been reported recently in hybrid systems where a metallic ferromagnet is exchanged biased by an organic film, and it is considered to be a spinterface effect. To understand this effect, we investigate if the molecular exchange bias exists in Co/metal tetra-phenyl porphyrin hybrid bilayer systems. Molecular exchange bias is never observed when the samples are properly encapsulated, and when exchange bias is eventually observed, it is not a spinterface effect, but it results from air-driven partial oxidation of the cobalt film transforming part of the metallic cobalt into a cobalt oxide that is well known to induce exchange bias effects. Surprisingly, oxidation is very difficult to prevent even by using very thick metallic encapsulating layers. A similar effect is observed in the Co/metal-phthalocyanine bilayer system showing that molecular exchange bias is not a spinterface effect also in the hybrid system in which this effect was originally discovered.

I. INTRODUCTION

Organic molecules are likely to play a major role and initiate breakthroughs in the field of molecular electronics by providing a new way to use the “spin” degree of freedom of the electron. Introducing small organic molecules in spintronics opened a new area of research called organic spintronics.¹ In theory, these molecules of low molecular weight are promising agents not only because of their strong electron-phonon coupling² and long spin coherence length, but also because of their different chemical functionalities which can open the possibility of combining several physical properties in a single device. The path from new concepts to the development of new devices was first explored at the turn of the 21st century when several groups reported the experimental evidence of direct spin-polarized injection and magnetoresistance effect in planar hybrid junction using hexa-thienyl (T_6) derivatives³ as well as low temperature giant magnetoresistance effects in vertical spin valve structure using small π conjugated 8-hydroxy-quinoline aluminum (Alq_3) molecules.⁴ Following these promising results, several spintronic effects were investigated in hybrid organic systems including the inverse spin-valve effect,^{5,6} tunneling magnetoresistance,^{7,8,9} magneto-transport,¹⁰ and other phenomena which are oriented towards spintronic device applications.

Many of these effects are interfacial phenomena which are highly dependent on the on-surface molecular behavior and on the metal-molecule interactions at the organic/inorganic interfaces. Sanvito introduced the science of “spinterface”¹¹ and Cinchetti et al. discussed the importance of tailoring and engineering the molecular interface.¹² One of the most interesting interfacial effects is related to the possibility of inducing magnetic moments at the organic/inorganic interfaces. Such effects occur because of the formation of hybrid π -d states at the interfaces that can induce new magnetic properties in the system. In this regard, C_{60} molecules are used extensively to study the influence of organic molecules on the magnetic properties of the ferromagnetic thin films at the metal/molecule interface.^{13,14,15} A second interesting implication of the spinterface science manifests itself directly in the change of the spin density of states at the Fermi energy, resulting in a sign inversion of the magnetoresistance in spin valve systems.¹⁶ More closely related to the topic investigated in this paper, a magnetic hardening effect is often observed in different organic/inorganic hybrid systems.^{17,18,19,20} The presence of interface magnetic hardening effect is associated to organic molecules in the chemisorption regime where the adsorbed molecules have strong interaction with the ferromagnetic substrate atoms and hence can locally modify the magnetic anisotropy of the surface atoms.

In this work we focused our investigations on a specific spinterface effect which is the molecular exchange bias. Indeed, exchange bias effect plays an important role in spintronic devices since it allows controlling the magnetization reversal process of a ferromagnetic film via interfacial exchange coupling with, usually, an adjacent anti-ferromagnetic layer. An initial report described how phthalocyanine (Pc) molecules in Co/MnPc bilayers induce an exchange bias on the cobalt (Co) film.²¹ The same effect has been reported with different metal phthalocyanine molecular layers,²² with metal octa-ethyl porphyrin bilayers^{23,24} and with a mono-layer of metal phthalocyanine molecules.²⁵ In these reports, the organic molecules have all a planar structure. Despite these promising results the presence of exchange bias in such organic/inorganic hybrid systems is rather surprising and remains controversial. To better understand the molecular exchange bias effect and the influence of the molecule’s planar character on the molecular exchange bias we have chosen to study a new family of organic molecules: metal tetra-phenyl porphyrin (MTPP).

In this work, several scenarios are explored addressing the presence of molecular exchange bias in different hybrid systems: Co/MTPP (M=Zn and Ni) and Co/CoPc. In all these systems, no molecular exchange bias is observed if the capping layer is thick enough and if the samples are measured right after being removed from the UHV deposition chamber in which they are built. However, after some time exposure to air the onset of molecular exchange bias is observed. Moreover, the strength of the exchange bias field further increases with time. The experimental protocol that we have used proves that the observed exchange bias in the studied organic systems is not an intrinsic spinterface effect at the molecule/ferromagnet interface but results from the partial oxidation of the Co film because of sample exposure to air. To understand these observations, atomic force microscopy (AFM) and X-ray photoelectron spectroscopy (XPS) techniques are employed. The oxidation mechanism is made possible because the Au capping film has, even for very large thickness, a discontinuous-island-like morphology rich in deep holes. Similar behavior is observed for Co/ZnTPP, Co/NiTPP, and Co/CoPc bilayers thus extending the conclusion to two different organic systems. With this work we can conclude that in Co/ZnTPP, Co/NiTPP (using Au and Cu buffer layers and Au and Cr capping layers), and even in Co/CoPc bilayer systems no molecular exchange bias is observed for properly encapsulated samples. While exchange bias does not exist in these systems, this does not mean that interface magnetic hardening is absent as well. Indeed, interface magnetic hardening can take place without resulting in exchange bias effects. This work also points out that such metal/organic systems can show tricky behaviors. However, the simple experimental protocol that has been used in this

report can be applied to any organic / metal hybrid system to check whether the observed phenomena are truly spinterface effects or simply result from the oxidation of the samples.

II. EXPERIMENTAL METHODS

Co/MTPP bilayers are prepared on Si/SiO₂ (500nm) substrates, on which a 25nm of Au buffer layer is deposited by electron beam deposition technique, in an ultra-high vacuum (UHV) molecular beam epitaxy (MBE) chamber with a base pressure of 1×10^{-9} mbar. After transfer of the samples to another UHV evaporation chamber, 6nm of Co is deposited by thermal evaporation with a flux of 0.16 Å/sec under deposition pressure of 2×10^{-9} mbar. After depositing the Co film, the samples are transferred without vacuum disruption to the organic molecular beam epitaxy chamber (OMBE) for the preparation of the above-mentioned molecular layers. High purity, in-lab synthesized ZnTPP and NiTPP molecules are sublimated (with no further purification) on top of the ferromagnetic Co film under 2×10^{-9} mbar deposition pressure and at a rate of 0.055 monolayer/sec (ML/sec) monitored with quartz. All layers in the heterostructures are prepared at room temperature and are capped with Au film to protect the samples from contamination. For the growth of CoPc, the molecules are purchased from a commercial source (Europhtal Industrial Pigments) and are further purified using gradient purification process before sublimation.

To check whether the Co film is not contaminated during the deposition of the MTPP molecules, two test Co films are prepared. One of the test samples is capped directly after the deposition of the Co film while the second one is introduced into the OMBE chamber. After MTPP started to sublime, the second test Co film is kept in the OMBE chamber during the same time as the regular samples, but the MTPP crucible shutter is kept closed. After removal from the OMBE chamber the sample is capped and its magnetization curve is compared to the one of the Co film directly capped after the Co deposition without being introduced into the OMBE chamber. The magnetization curves of the two samples are very similar. This measurement shows that the sublimation of MTPP molecules in the UHV chamber does not result in the oxidation of the Co film surface.

After preparation of the heterostructures, the samples are transferred to an ex-situ AFM (Bruker Icon AFM), to a SQUID magnetometer (MPMS3, Quantum Design Inc), and to a XPS chamber for morphological, magnetic, and chemical element-specific characterizations. AFM scans are conducted in normal tapping mode under ambient conditions and AFM images are processed with WSxM 4.0 Beta 9.3²⁶ image processing software. The magnetic characterizations are conducted with SQUID by applying an in-plane magnetic field and the magnetic hysteresis loops are acquired at 2K after the samples are field cooled in an external static magnetic field.

The XPS measurements are performed in an UHV chamber spectrometer equipped with a RESOLVE 120 MCD5 hemispherical electron analyzer. Al K_α, $h\nu = 1486.6$ eV dual anode X-ray source is used as an incident radiation. Constant pass energy mode is used to record both survey and high-resolution spectra with pass energies of 50 and 20 eV, respectively. Curve fitting is performed using the CasaXPS 2.3.23 software with a mixed Gaussian/Lorentzian function for the full width at half maximum (FWHM) of the peaks.

The X-ray diffraction patterns show that the Au films have a face centered cubic (fcc) structure with a [111] growth direction, and that the Co films have a hexagonal close packed (hcp) structure with a [002] growth direction. The structure of the Co films is further investigated by ferromagnetic nuclear resonance (FNR; nuclear magnetic resonance for ferromagnets).²⁷ The observed spectra are consistent with hcp Co having a magnetization direction perpendicular to the hcp c-axis²⁸ as expected for an in-

plane magnetized hcp [0001] Co film. The quantitative analyses of the FNR spectra revealed an fcc Co content of about 30% (see supplementary Fig. S4(b)). Detailed FNR analyses will be published elsewhere.

To check if the deposited molecules are not damaged by the sublimation process, the UV-Vis absorbance spectra of ZnTPP, NiTPP and CoPc films have been recorded (Fig. S5). These spectra allow to confirm that the sublimated organic molecules have the same optical properties as the ZnTPP, NiTPP and CoPc bulk compounds.

III. RESULTS AND DISCUSSION

The first hybrid samples investigated are built with zinc metallated TPP molecules (ZnTPP). ZnTPP molecules are diamagnetic with Zn(II) closed shell central-ion and they have weak van der Waals interactions with the metallic surfaces.²⁹ Therefore, ZnTPP molecules are more likely to be insensitive to the proximity of the Co layer. Before measuring the magnetization loop of the full stack hybrid samples, the behavior of the Co film in the Au(25nm)/Co(6nm)/Au(10nm) stack is used as a reference for comparison with the Co/MTPP and Co/CoPc hybrid samples. The magnetization loop of the reference sample depicted in Fig. 1(a) shows a symmetrical loop with $|H_{c1}| = |H_{c2}| = 100$ Oe. This magnetization curve is stable with time (on a timescale of several months) which shows that 10nm of Au capping layer is thick enough to protect the metallic Co from surface oxidation.

The magnetization loop obtained for the Co(6nm)/ZnTPP(10nm) samples capped with 10nm of Au are shown in Fig. 1(b). The sample is measured directly after being removed from the UHV chamber. Rather surprisingly the Co(6nm)/ZnTPP(10nm) bilayer sample (Fig. 1(b), black loop) exhibits exchange bias with a clear shift in its hysteresis loop towards the negative field axis. The exchange bias field is $H_{EB} = -260$ Oe. In addition to exchange bias, the saturation magnetization of the system shows a significant decrease compared to the saturation magnetization value of the reference sample. It is 33% smaller than the one of the reference sample.

Following this issue, the magnetic behavior of the same sample is tracked over several weeks while keeping the sample in a standard desiccator. Its magnetization loop is measured again after 2 months. As seen in Fig. 1(b), the magnetization loop (red curve) of the aged sample shows a further loss in saturation magnetization with a strong increase in the coercive fields. The resulting exchange bias field increased to $H_{EB} = -600$ Oe. Several reasons may explain the increase in the exchange bias field. First, the exchange bias effect in such hybrid organic systems is supposed to originate from the interface-induced magnetization in the organic layer that creates pinning sites for the ferromagnetic Co film. These pinning sites might increase with time and therefore exert a larger exchange field on the Co film. Similarly, the magnetic hardening effect might also evolve with time. However, in a previous report we show that there is no magnetic hardening occurring at the Co/ZnTPP interfaces as the hybrid interfaces are magnetically softer than the bulk part of the Co film.²⁹ Finally, and more trivially, although we show that 10nm of Au capping layer is thick enough to protect the reference sample it is possible that the same Au(10nm) capping layer is not thick enough to protect the bilayer samples leading to their contamination due to exposure to air. This exposure to air might lead to the partial oxidation of the Co film resulting in an exchange coupling between the remaining metallic Co layer and newly formed cobalt oxide (CoO).³⁰ The extent of the Co film's oxidation might simply increase with time.

To address the efficiency of the Au capping layer, the thickness of the capping layer is increased to 50nm keeping the rest of the heterostructure similar to the previous sample: Si/SiO₂/Au(25nm)/Co(6nm)/ZnTPP(10nm)/Au(50nm). The magnetization loops of the 50nm capped

hybrid samples are presented in Fig. 1(c). Remarkably, the freshly prepared Co(6nm)/ZnTPP(10nm) bilayer sample capped with 50nm of Au shows a symmetrical hysteresis loop with no evidence of exchange bias (Fig. 1(c)), black curve). However, after 2 weeks while the sample is intentionally kept at room atmosphere, a shift in its hysteresis loop with $H_{EB} = -510 \text{ Oe}$ (Fig. 1(c), red curve) is observed. The onset of this bias is rather surprising since the Au(50nm) capping layer is much thicker than the Co(6nm) and ZnTPP(10nm) films and should properly encapsulate the samples. It can be highlighted that such thick capping layer is seldom used in other published works. While these results strongly suggest that despite such thick capping layer, the Co layer becomes partly oxidized, they do not completely rule out the possibility that a solid-state chemical reaction with a slow kinetic of weeks' time scale might take place at the organic/metal interface.

As an ultimate check, the same heterostructure Si/SiO₂/Au(25nm)/Co(6nm)/ZnTPP(10nm)/Au(50 nm) is again prepared but this time the sample is kept in the UHV chamber for 2 complete weeks with no exposure to air until the time of measurement. The sample has a very similar magnetic behavior (Fig. 1(d)) to the previous sample that was not kept in UHV for 2 weeks (Fig. 1(c), black curve). The magnetization loop shows perfectly symmetric response with no shift at all. This last experimental procedure shows that the exchange bias is never observed prior to the air exposure of the sample. Therefore, the presence of exchange bias can only be attributed either to the direct partial oxidation of the Co films or to an atmosphere mediated solid-state reaction at the metal/organic interface.

From these investigations it is clear that diamagnetic ZnTPP molecules cannot induce the molecular exchange bias. An alternate MTPP molecule has been investigated: NiTPP. Compared to the Zn(II) free ion that has a closed shell with a $3d^{10}$ configuration, the Ni(II) free ion has an open shell with a $3d^8$ configuration. However since the Ni(II) ion site symmetry in NiTPP is D_{4h} the molecule shows a diamagnetic behavior³¹ like the ZnTPP molecule. NiTPP also has the advantage of being more stable than ZnTPP. The increased stability of NiTPP results from the atomic radius of the Ni atom (163pm) compared to Zn (139pm), thus the Ni cation has stronger single chemical bonds with the four nitrogen atoms within the core of the porphyrin macrocycle.

The sample is directly grown with a thick Au capping layer (Si/SiO₂/Au(25nm)/Co(6nm)/NiTPP(10nm)/Au(50nm)) and the magnetization loop of the “freshly deposited” sample is recorded right after sample preparation and measured again after 1 week while the sample is intentionally exposed to air. Its hysteresis loops are shown in Fig. 2. The “freshly deposited” sample (Fig. 2, black loop) has a symmetrical magnetization loop with respect to the field origin and zero exchange bias field. Its shape is very similar to the one observed for the ZnTPP samples measured directly after being removed from the UHV chamber (fig. 1 (c) and (d)). After 1 week, a more interesting magnetization loop is observed (Fig. 2, red loop) with two different reversals at different field ranges. This hints at the presence of different magnetic domains with different magnetic anisotropies in the ferromagnetic Co film. One part of the sample reverses at small fields ($|H_{c1 \text{ soft}}| = |H_{c2 \text{ soft}}| = 100 \text{ Oe}$) and shows no exchange coupling. The second part shows an asymmetrical reversal at higher fields and with a small shift towards the negative field axis in the hysteresis loop which indicates the onset of exchange bias in these domains ($H_{EB} = -70 \text{ Oe}$). However, the main result is that the properly capped and “freshly deposited” sample does not show any molecular exchange bias.

The investigations conducted on Co/ZnTPP and Co/NiTPP samples allow concluding that the molecular exchange bias in these Co/MTPP hybrid systems is not a spinterface effect but is more trivially due to the air-driven partial oxidation of the Co film or to an air mediated solid-state reaction at the interface.

Surprisingly even a Au capping layer as thick as 50nm is still not large enough to protect the samples on a time scale larger than few days.

In order to understand if the exchange bias originates from the partial oxidation of the Co film or from an air mediated solid-state reaction at the interface, AFM studies and XPS investigations are performed to reveal the morphological characteristics of the topmost Au capping layer and to probe the chemical species of the buried layers, respectively.

Fig. 3 represents the $Co\ 2p_{3/2}$ XP spectra of the CoTPP compound, of the uncapped Au(25nm)/Co(6nm) reference sample which shows exchange bias (see supplementary Fig. S1) and of the aged Au(25nm)/Co(6nm)/ZnTPP(10nm)/Au(10nm) hybrid sample. In Fig. 3(a), the black spectrum representing the $Co\ 2p_{3/2}$ signal of the uncapped Au(25nm)/Co(6nm) reference sample, and the red spectrum representing the $Co\ 2p_{3/2}$ signal of the aged Au(25nm)/Co(6nm)/ZnTPP(10nm)/Au(10nm) hybrid sample, show exactly the same two main peaks: a first peak at binding energy of 778.1 eV which corresponds to Co(0) for metallic Co³² and a second peak at 781.1 eV attributed to CoO and Co₃O₄ structures.^{33,34,35} The similarity of the two spectra is consistent with our hypothesis that the Co film in the Au(25nm)/Co(6nm)/ZnTPP(10nm)/Au(10nm) hybrid sample is partially oxidized.

In addition, the spectrum of the reference CoTPP powder is shown in Fig. 3(b). It has a sharp main peak at 780.1 eV that is typical for Co(II) peak in the molecule^{36,37} and a much broader and weaker shoulder at around 782 eV. This shoulder is a multiplet structure of the signal which is due to the unpaired electrons of the d^7 shell of the Co(II) within the molecule and is in good agreement with previously reported experimental and theoretical works.^{36,38} It is important to note that no contribution is observed in the range of 780.1 eV in the spectrum of the aged Au(25nm)/Co(6nm)/ZnTPP(10nm)/Au(10nm) hybrid sample (Fig. 3(a), black spectrum) which shows that the Zn(II) ion of the molecule is not being replaced by the Co metallic atoms of the Co film when the ZnTPP molecules are adsorbed on the Co surface.

Moreover, Fig. 4 shows the $N\ 1s$ and $Zn\ 2p_{3/2}$ XP spectra of the aged Co(6nm)/ZnTPP(10nm)/Au(10nm) hybrid sample, and of the ZnTPP and CoTPP powders. The dark blue line of Fig. 4(a) represents the fitted spectrum of the $N\ 1s$ signal acquired from the aged Co(6nm)/ZnTPP(10nm)/Au(10nm) hybrid sample. In this spectrum, the observed peaks are analysed in three-peak component. The first peak is at 398.6 eV and lies in the binding energy range of the four aminic nitrogen atoms bonded to the Zn(II) ion within the molecule. A second peak appears at 400.1 eV and could result from the pyrrolic nitrogen in the porphyrin compound that has a single bond with the hydrogen atom. Finally, a third peak of low intensity appears at higher binding energies (402.2 eV) that corresponds to charged nitrogen moieties.³⁹

Fig. 4(b) shows the $N\ 1s$ spectrum of ZnTPP powder in which the observed peak is also analyzed in component to show the possible differences with the corresponding peaks observed in the spectrum of the aged Co(6nm)/ZnTPP(10nm)/Au(10nm) sample. In the ZnTPP powder's spectrum, there is a main, narrow peak at 398.3 eV which corresponds to the four aminic nitrogens of the molecule, and a high binding energy component of drastically lower intensity. The difference in the $N\ 1s$ spectra-shape of the aged Co/ZnTPP sample and the ZnTPP compound could result from the deposition of the top-most Au capping layer. This is because it is possible that the metallic atoms (in our case Au adatoms) deposited on top of soft organic films might partly diffuse into the organic film and intermix or chemically react with the molecules of the organic film.

However, in Fig. 4(c), the $Zn\ 2p_{3/2}$ red XP spectrum of the aged Co(6nm)/ZnTPP(10nm)/Au(10nm) hybrid sample shows only one main peak at 1021.9 eV which corresponds to Zn(II) ion of the molecule in the multilayer regime.^{36,37} This peak is very close to the Zn(II) ion peak observed in the $Zn\ 2p_{3/2}$ spectrum of ZnTPP powder (Fig. 4(c) black spectrum) and suggests that Zn(II) ion-sites of the molecules are most likely not hindered by the incoming Au adatoms.

The XPS analyses allow concluding that the peak at 781.1 eV in the $Co\ 2p_{3/2}$ spectrum of the aged Au(25nm)/Co(6nm)/ZnTPP(10nm)/Au(10nm) hybrid sample is due to the air-driven partial oxidation of the Co film. It confirms that the partial oxidation of the Co film is at the origin of the exchange bias observed in the studied hybrid samples.

Actually, XPS also indirectly revealed that a thickness of 10nm for the Au capping layer is not large enough to efficiently protect the samples from air induced oxidation. Indeed, a layer thickness of 10nm is already very thick compared to the XPS electron escape length and no XPS signal should be detected from the inner layers if this capping layer would have a continuous morphology with a homogeneous thickness. The fact that XPS signals could be easily recorded shows that a significant surface area of the samples is covered with only a very thin layer of Au, if any at all.

Finally, to get a direct insight into the surface-morphology of the sample the surface of the Au(10nm) capping layer of the aged Au(25nm)/Co(6nm)/ZnTPP(10nm) hybrid sample is studied with AFM. Supplementary Fig. S3 presents the surface morphology image of the 10nm Au capping layer scanned at $3\mu m$ scan size. Indeed, the surface has discontinuous morphology. It is composed of un-patterned, elongated worm-like disconnected islands separated by darker contrasts which are typical signatures of deep cracks. The surface RMS roughness is $\sigma_{RMS} \approx 7nm$. The height profile of the Au(10nm) capping layer's surface clearly illustrates that these cracks go as deep as 25nm and are extended over a width of the order of 200nm. Such poor morphology of the sample could be considered one of the main reasons for the oxidation of the Co films. The deep cracks probably extend down to the Co film allowing the ingress of oxygen.

From this study it is clear that the Co/MTPP hybrid systems do not show molecular exchange bias. However, this could result from a bad choice of buffer and/or capping layers. To check this point, the measurements were repeated using a Cu buffer layer and a Cr capping layer (see supplementary information fig. S6 and S7). Samples with thinner Co layer thickness have also been measured (fig. S8). All freshly deposited samples did not show any exchange bias. In addition, the Cr capping layer revealed to be very efficient, and the onset of exchange bias is not observed even after several months from sample preparation (fig. S7).

This study raised one important question about the Co/MPc systems in which the molecular exchange bias has been initially observed: does the reported molecular exchange bias really originate from the exchange field due to the organic molecules? At the light of the results obtained on the Co/MTPP systems, we decided to reproduce the study with the Co/CoPc system. CoPc molecules are paramagnetic with $S = \frac{1}{2}$ and have a Co(II) magnetic central ion.

The Co/CoPc bilayers are grown using the same procedure as in ref. 22 and have the following sample stack: Si/SiO₂/Co(10nm)/CoPc(10nm)/Au(10nm). The CoPc thickness that has been used is the thickness for which the exchange bias is maximum in ref. 21. SQUID measurements are conducted using the same methodology as for the Co/MTPP/Au samples and the magnetometry results of the Co/CoPc samples are presented in Fig. 5. The magnetization loop of the “freshly deposited” Co(10nm)/CoPc(10nm) hybrid sample capped with 10nm of Au has a symmetrical loop showing no hints of exchange bias. However, already after 5 days of intentional exposure to air (Fig. 5(a), red loop),

a loss in magnetization is observed and exchange bias appears with a magnitude of $H_{EB} = -352 \text{ Oe}$. Finally, the Co(10nm)/CoPc(10nm) sample capped with 10nm Au shows no onset of molecular exchange bias when kept in the UHV chamber for several days before measurement. Therefore, it can be concluded that, as with the MTPP molecules, the molecular exchange bias in this Co/CoPc hybrid system is also the consequence of the partial oxidation of the Co films that occurs when the samples are exposed to air for ex-situ measurements.

IV. CONCLUSION

For developing the next generation of fully organic devices, molecular exchange bias, if existing, could have a huge impact on implementing mechanically soft and environment friendly devices. To understand the origin of this spinterface effect, we investigated the existence of molecular exchange bias in Co/MTPP and Co/CoPc bilayer systems. Our investigations revealed that when the capping layer is thick enough, the samples directly measured after being removed from the UHV chamber consistently do not show any molecular exchange bias effect. It is only after the samples have been exposed to air during some time (few hours to several weeks, depending on the capping layer thickness) that the onset of exchange bias is observed. Finally, when the same samples are kept in an UHV chamber for several weeks they never show any sign of exchange bias prior to air exposure. This simple experimental protocol suggests that in all the samples we have investigated, when exchange bias is observed, it is induced by the air-driven partial oxidation of the Co film, and it is not a spinterface effect. This is confirmed by using alternate buffer and capping layers. This hypothesis is supported with AFM and XPS measurements which show that the partial oxidation of the Co films is made possible because of the poor efficiency of the capping layers even when the Au capping layer is as thick as 50nm. These observations point out that such organic/metal systems can show tricky behaviors. However, the simple experimental protocol that has been used in this work can be applied to any organic/metal hybrid system in order to check if the observed phenomena are truly spinterface effects or result from the oxidation of the samples. This work also demonstrates that new experimental approaches have to be developed to probe the stacking quality of such organic/inorganic hybrid heterostructures.^{29, 40}

SUPPLEMENTARY MATERIAL

See supplementary material for additional magnetization curves of samples with alternate capping layers and Co thickness. Additional data about the structural and morphological characterisations of the films are also shown.

ACKNOWLEDGEMENTS

This work of the Interdisciplinary Thematic Institute QMat, as part of the ITI 2021-2028 program of the University of Strasbourg, CNRS and Inserm, was supported by IdEx Unistra (ANR-10-IDEX-0002), by SFRI STRAT'US project (ANR-20-SFRI-0012), and by ANR-11-LABX-0058_NIE under the framework of the French Investments for the Future Program. We acknowledge Christophe Kieber for technical assistance and the "Initiative d'Excellence" (IdEx, excellence beyond borders) program of the University of Strasbourg for scholarship to Garen Avedissian.

DATA AVAILABILITY

The data that support the findings of this study are available from the corresponding author upon reasonable request.

REFERENCES

- ¹J. S. Moodera, B. Koopmans, and P. M. Oppeneer, *MRS Bull.* **39**, 578 (2014).
- ²V. Coropceanu, J. Cornil, D. A. da Silva Filho, Y. Olivier, R. Silbey, and J. L. Bredas, *Chem. Rev.* **107**, 926 (2007).
- ³V. Dediu, M. Murgia, F. C. Matacotta, C. Taliani, and S. Barbanera, *Solid State Commun.* **122**, 181 (2002).
- ⁴Z. H. Xiong, D. Wu, Z. V. Vardeny, and J. Si, *Nature.* **427**, 821 (2004).
- ⁵A. Riminucci, I. Bergenti, L. E. Hueso, M. Murgia, C. Taliani, Y. Zhan, F. Casoli, M. P. de Jong, and V. Dediu, *arXiv:cond-mat/0701603*.
- ⁶F. J. Wang, C. G. Yang, Z. V. Vardeny, and X. G. Li, *Phys. Rev. B* **75**, 245324 (2007).
- ⁷W. Xu and G. J. Szulczewski, *Appl. Phys. Lett.* **90**, 072506 (2007).
- ⁸H. Vinzelberg, J. Schumann, D. Elefant, R. B. Gangineni, J. Thomas, and B. Bucher, *J. Appl. Phys.* **103**, 093720 (2008).
- ⁹M. Grünewald, M. Wahler, F. Schumann, M. Michelfeit, C. Gould, R. Schmidt, F. Würthner, G. Schmidt, and L. W. Molenkamp, *Phys. Rev. B* **84**, 125208 (2011).
- ¹⁰C. Barraud, K. Bouzehouane, C. Deranlot, D. J. Kim, R. Rakshit, S. Shi, J. Arabski, M. Bowen, E. Beaupre, S. Boukari, F. Petroff, P. Seneor, and R. Mattana, *Dalton Trans.* **45**, 16694 (2016).
- ¹¹S. Sanvito, *Nat. Phys.* **6**, 562 (2010).
- ¹²M. Cinchetti, V. Dediu, and L. E. Hueso, *Nat. Mater.* **16**, 507 (2017).
- ¹³K. Bairagi, A. Bellec, V. Repain, C. Chacon, Y. Girard, Y. Garreau, J. Lagoute, S. Rousset, R. Breitwieser, Y. -C. Hu, Y. C. Chao, W. W. Pai, D. Li, A. Smogunov, and C. Barreteau *Phys. Rev. Lett.* **114**, 247203 (2015).
- ¹⁴T. L. A. Tran, P. K. J. Wong, M. P. de Jong, W. G. van der Wiel, Y. Q. Zhan, and M. Fahlman. *Appl. Phys. Lett* **98**, 222505 (2011).
- ¹⁵T. Lan Anh Tran, D. Çakır, P. K. Johnny Wong, A. B. Preobrajenski, G. Brocks, W. G. van der Wiel, and M. P. de Jong, *ACS Appl. Mater. Interfaces* **5**, 837 (2013).
- ¹⁶A. Bedoya-Pinto, S. G. Miralles, S. Vélez, A. Atxabal, P. Gargiani, M. Valvidares, F. Casanova, E. Coronado, and L. E. Hueso, *Adv. Funct. Mater.* **28**, 1702099 (2018).
- ¹⁷T. Moorsom, M. Wheeler, T. M. Khan, F. Al Ma’Mari, C. Kinane, S. Langridge, D. Ciudad, A. Bedoya-Pinto, L. Hueso, G. Teobaldi, V. K. Lazarov, D. Gilks, G. Burnell, B. J. Hickey, and O. Cespedes, *Phys. Rev. B* **90**, 125311 (2014).

- ¹⁸M. Callsen, V. Caciuc, N. Kiselev, N. Atodiresei, and S Blügel, Phys. Rev. Lett. **111**, 106806 (2013).
- ¹⁹K. Bairagi, A. Bellec, V. Repain, C. Fourmental, C. Chacon, Y. Girard, J. Lagoute, S. Rousset, L. Le. Laurent, A. Smogunov, and C. Barreteau, Phys. Rev. B **98**, 085432 (2018).
- ²⁰K. V. Raman, A. M. Kamerbeek, A. Mukherjee, N. Atodiresei, T. K. Sen, P. Lazić, V. Caciuc, R. Michel, D. Stalke, S. K. Mandal, S. Blügel, M. Münzenberg, and J. S. Moodera, Nature **493**, 509 (2013).
- ²¹M. Gruber, F. Ibrahim, S. Boukari, H. Isshiki, L. Joly, M. Peter, M. Studniarek, V. Da Costa, H. Jabbar, V. Davesne, U. Halisdemir, J. Chen, J. Arabski, E. Otero, F. Choueikani, K. Chen, P. Ohresser, W. Wulfhekel, F. Scheurer, W. Weber, M. Alouani, E. Beaurepaire, and M. Bowen, Nat. Mater. **14**, 981 (2015).
- ²²S. Boukari, H. Jabbar, F. Schleicher, M. Gruber, G. Avedissian, J. Arabski, V. Da Costa, G. Schmerber, P. Rengasamy, B. Vilen, W. Weber, M. Bowen, and E. Beaurepaire, Nano Lett. **18**, 4659 (2018).
- ²³J. Jo, J. Byun, I. Oh, J. Park, M. J. Jin, B. C. Min, J. Lee, and J. -W. Yoo, ACS Nano, **13**, 894 (2019).
- ²⁴J. Jo, J. Byun, J. Lee, D. Choe, I. Oh, J. Park, M. -J. Lee, J. Lee, and J. -W. Yoo, Adv. Funct. Mater. **1908499** (2020).
- ²⁵S. Mundlia, S. Chaudhary, L. Peri, A. Bhardwaj, J. J. Panda, S. Sasmal, and K. V. Raman, Phys. Rev. Appl. **14**, 024095 (2020).
- ²⁶I. Horcas, R. Fernandez, J. M. Gomez-Rodriguez, J. Colchero, and J. Gomez-Herrero, Rev. Sci. Instrum. **78**, 013705 (2007).
- ²⁷C. Meny and P. Panissod, Annual Reports on NMR Spectroscopy **103**, 47 (2021).
- ²⁸M. Malinowska, C. Meny, E. Jedryka, and P. Panissod, J. Phys. Condens. Matter. **10**, 4919 (1998).
- ²⁹G. Avedissian, J. Arabski, J. A. Wytko, J. Weiss, and C. Meny, Phys. Rev. B **102**, 184114 (2020).
- ³⁰W.H. Meiklejohn and C. P. Bean, Phys. Rev. **102**, 1413 (1956).
- ³¹C. Wäckerlin, K. Tarafder, J. Girovsky, J. Nowakowski, T. Hählen, A. Shchyrba, D. Siewert, A. Kleibert, F. Nolting, P. M. Oppeneer, T. A. Jung and N. Ballav, Angew. Chem. Int. Ed. **52**, 4568 (2013).
- ³²C. D. Wagner, W. M. Riggs, L. E. Davis, J. F. Moulder, and G. E. Muilenberg, Perkin Elmer Corp. Publisher, Eden Prairie, MN, (1979).
- ³³S. C. Petitto and M. A. Langell, J. Vac. Sci. Technol. A **22**, 1690 (2004).
- ³⁴T. J. Chuang, C. R. Brundle, and D. W. Rice, Surf. Sci. **59**, 413 (1976).
- ³⁵S. Xie, Y. Liu, J. Deng, J. Yang, X. Zhao, Z. Han, K. Zhang, and H. Dai, J. Catal. **352**, 282 (2017).
- ³⁶T. Lukasczyk, K. Flechtner, L. R. Merte, N. Jux, F. Maier, J. M. Gottfried, and H. P. Steinruck, J. Phys. Chem. C, **111**, 3090 (2007).
- ³⁷L. Scudiero, D. E. Barlow, and K. W. Hipps, J. Phys. Chem. B, **104**, 11890 (2000).
- ³⁸R. P. Gupta and S. K. Sen, Phys. Rev. B **12**, 15 (1975).
- ³⁹E. Desimoni and B. Brunetti, Chemosensors **3**, 70 (2015).
- ⁴⁰G. Avedissian, J. Arabski, J. A. Wytko, J. Weiss, and C. Meny, Adv. Funct. Mater. **30**, 2005605 (2020).

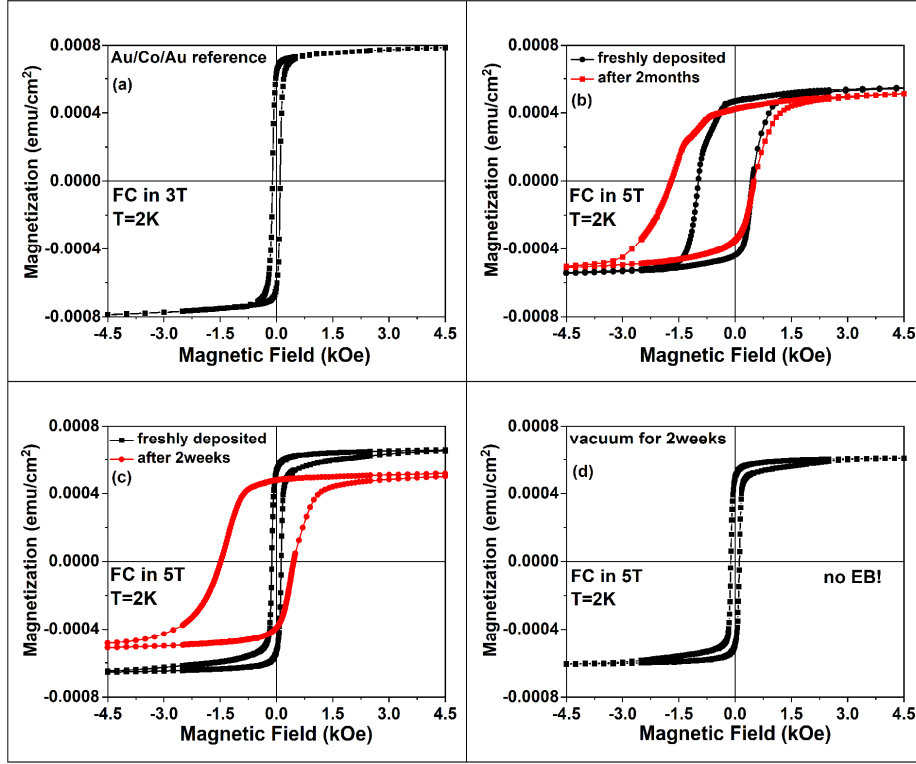


FIG.

1. Magnetization loop of (a) Au(25nm)/Co(6nm)/Au(10nm) reference sample after field cooling in +3T external field (b) Co(6nm)/ZnTPP(10nm)/Au(10nm) bilayer sample, "freshly deposited" (black) and measured after 2 months (red) (c) Co(6nm)/ZnTPP(10nm)/Au(50nm) bilayer sample, "freshly deposited" (black); measured after 2 weeks (red) (d) fresh "as deposited" Co(6nm)/ZnTPP(10nm)/Au(50nm) bilayer sample kept under UHV for 2 weeks. The hybrid samples are field cooled in +5T in-plane external field and the loops are acquired at T=2K.

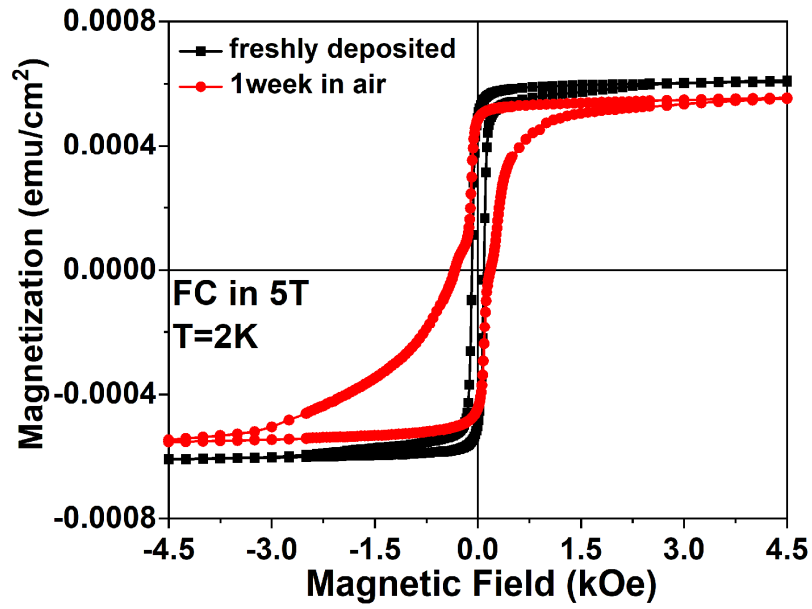


FIG. 2. Magnetization loop of Co(6nm)/NiTPP(10nm)/Au(50nm) bilayer, “freshly deposited” (black) and after 1 week of exposure to air (red). Measurements are conducted at 2K after field cooling the samples in +5T in-plane external field.⁷

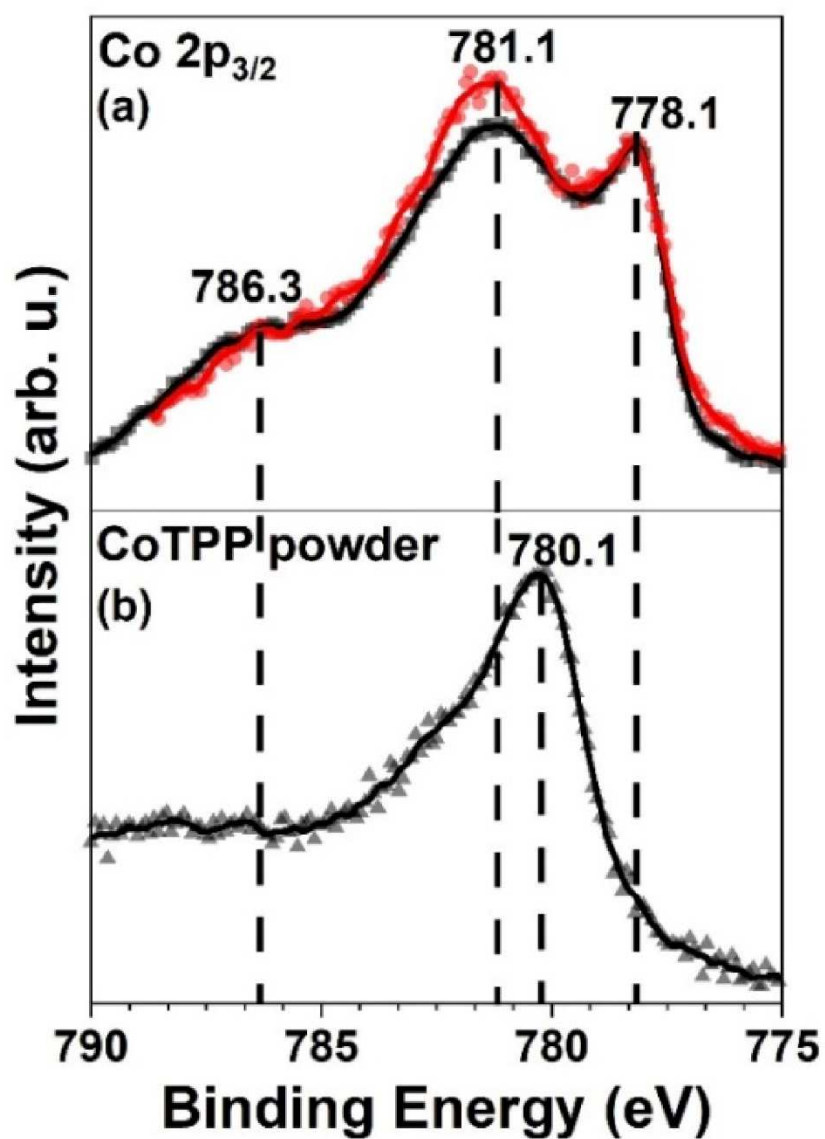


FIG. 3. *Co 2p_{3/2}* XPS spectra of (a) Au(25nm)/Co(6nm) uncapped reference sample (black) and of Co(6nm)/ZnTPP(10nm)/Au(10nm) hybrid sample (red), (b) Co(II)TPP compound. Scattered points are the raw data, and the bold lines are the smoothed spectra. A satellite peak is present at 786.3 eV for all spectra, and it results from the multi electron excitation process during a photoemission mechanism.

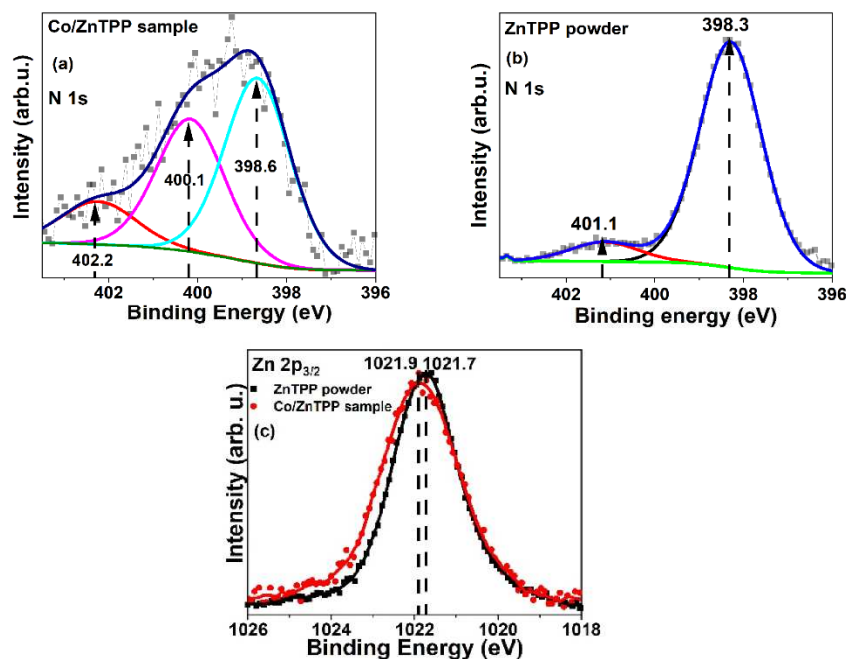


FIG. 4. (a) $N\ 1s$ XPS experimental spectrum of the aged Co(6nm)/ZnTPP(10nm)/Au(10nm) sample in scattered points and the corresponding fittings in full lines. (b) $N\ 1s$ XP spectrum of the ZnTPP compound. (c) $Zn\ 2p_{3/2}$ XPS spectra of the ZnTPP compound (black) and of aged Co(6nm)/ZnTPP(10nm)/Au(10nm) sample (red).

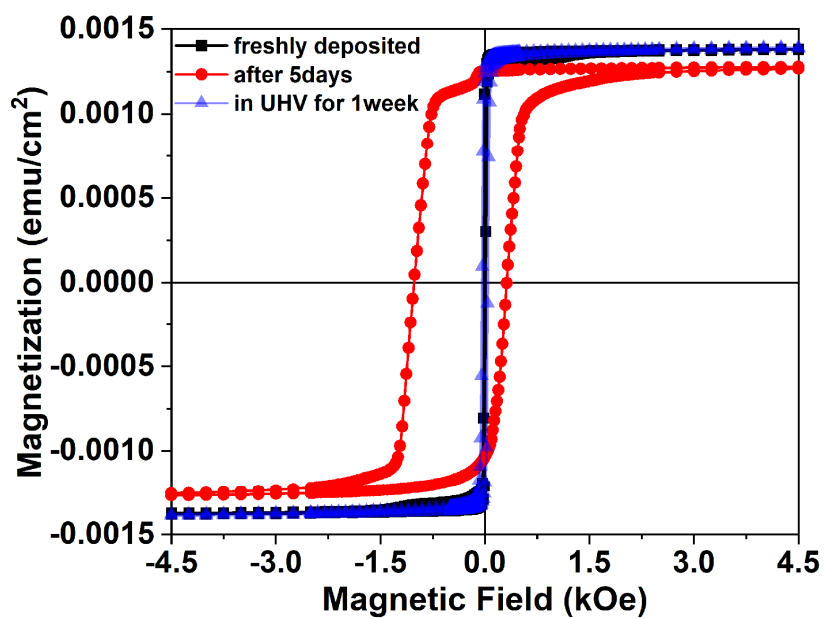


FIG. 5. Magnetization loop of the “freshly deposited” Co(10nm)/CoPc(10nm)/Au(10nm) hybrid sample (black loop), of the same sample measured again after 5 days in air (red loop) and of a similar Co(10nm)/CoPc(10nm)/Au(10nm) sample (blue loop) after being kept in a UHV chamber for 1 week.